Letters

Demonstration of Avalanche and Surge Current Robustness in GaN Junction Barrier Schottky Diode With 600-V/10-A Switching Capability

Feng Zhou, *Student Member, IEEE*, Weizong Xu, *Member, IEEE*, Fangfang Ren, Dong Zhou, Dunjun Chen, Rong Zhang, Youdou Zheng, Tinggang Zhu, and Hai Lu, *Senior Member, IEEE*

***Abstract*—In this letter, we achieved significantly enhanced avalanche ruggedness and surge current capability in GaN junction barrier Schottky (JBS) diode for highly reliable power operation. Based on the selective Mg-ion implantation technology, the GaN JBS diode obtains superior electrostatic performances, including 830-V breakdown voltage, 150-mΩ specific ON-state resistance, and 0.5-V turning ON voltage. Meanwhile, zero reverse recovery behaviors are observed even under extreme switching conditions of 600 V/10 A. During the reliability evaluation in the inductive load circuits, crucial avalanche capability with avalanche breakdown voltage over 965 V, avalanche energy up to 57.8 mJ, and more than 10 000 repetitive avalanche breakdown events are demonstrated. Together with the surge current tolerance up to 65 A and surge energy of 6.0 J, a large safe-operation-area under both forward and reverse inductive spikes is realized for the GaN-based rectifier.**

***Index Terms*—Avalanche breakdown, GaN, junction barrier Schottky (JBS) diode, safe-operation-area (SOA), surge current.**

I. Introduction

TRANSIENTS, i.e., momentary spikes in voltage or current, which generally couples from lightning, electrostatic discharge, and circuits experiencing a sudden change due to a switch opening or a short occurring, can disrupt or damage the electronic devices connected to signal or power lines. This situation deteriorates in power systems, where power devices are operating under critical conditions of high voltage and large current. Therefore, power devices with robustness against transients are the essential part in power modules for safe operation.

Manuscript received February 5, 2021; revised April 8, 2021; accepted April 26, 2021. Date of publication April 29, 2021; date of current version July 30, 2021. This work was supported in part by the National Key R&D Program of China under Grant 2017YFB0403000 and in part by the National Natural Science Foundation of China under Grants 61921005 and 62004099. *(Corresponding authors: Weizong Xu; Hai Lu.)*

Feng Zhou, Weizong Xu, Fangfang Ren, Dong Zhou, Dunjun Chen, Rong Zhang, Youdou Zheng, and Hai Lu are with the School of Electronic Science and Engineering, Collaborative Innovation Center of Advanced Microstructures, Nanjing University, Nanjing 210093, China (e-mail: dg1923060@smail.nju.edu.cn; wz.xu@nju.edu.cn; ffren@nju.edu.cn; dongzhou@nju.edu.cn; djchen@nju.edu.cn; rzhang@nju.edu.cn; ydzheng@nju.edu.cn; hailu@nju.edu.cn).

Tinggang Zhu is with the CorEnergy Semiconductor Company Ltd., Suzhou 215000, China (e-mail: gavin@corenergy.com).

Color versions of one or more figures in this article are available at https://doi.org/10.1109/TPEL.2021.3076694.

Digital Object Identifier 10.1109/TPEL.2021.3076694

Nowadays, gallium nitride (GaN) based power devices have invoked great interest for high-frequency and high-efficiency power applications [1]. The attractive properties of GaN, including wide bandgap, high breakdown electric field, and high electron mobility, boast GaN as competitive candidate for the next-generation power devices [2], [3]. Among the GaN power rectifiers, the vertical GaN Schottky barrier diode (SBD) can deliver lower conduction/switching losses and higher switching frequency, owing to its lower forward voltage and faster reverse recovery behavior [4], [5]. Despite the inspiring material attributes and outstanding performance, the reliability of GaN technology is still a major hurdle to its widespread market adoption [6]. Especially, the device performances under momentary spikes that could lead to critical breakdown or current surge have large research significances [6]–[8]. As has been demonstrated in Si and SiC power devices, rugged avalanche capability that dissipates transient energy via impact ionization without triggering destructive breakdown, and a strong surge current tolerance in forward conduction, largely determines the robustness and safe-operation-area (SOA) of the power device against transients [9], [10]. Thus, the avalanche breakdown and surge current characteristics in GaN device with relatively more severe reliability concerns worth specific investigations [11], [12].

Recent advances in the reliability of GaN-based rectifiers show certain success in p–n diodes (PNDs), achieving a high avalanche energy of ∼60 mJ and a surge current of ∼10 A [13], [14]. However, GaN SBDs have encountered a more difficult path to achieve reliable operation. The electric field spike near Schottky contact edge and the leakage path along the dislocations [15], as well as the severe thermal budget under high-power operation could result in large leakage current and poor breakdown voltage (*BV*) [4], [5]. In this letter, p-GaN islands with micrometer spacing are produced underneath the anode contact, forming a junction barrier Schottky (JBS) like structure, which is effective to push the peak electrical field away from the metal/semiconductor contact interface and suppress reverse leakage current [16]–[18].

Correspondingly, the diode exhibit impressive dc performances and zero reverse recovery behavior under 600-V/10-A switching conditions, providing qualified device for the circuit-level reliability evaluation, which is indispensable for the final

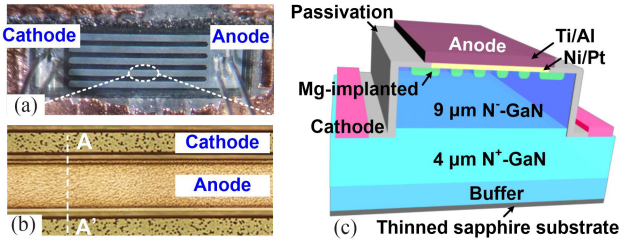

Fig. 1. (a) Optical microscope image and (b) zoomed-in multifinger region of the GaN JBS diode. (c) 3-D cross-sectional view along line AA'.

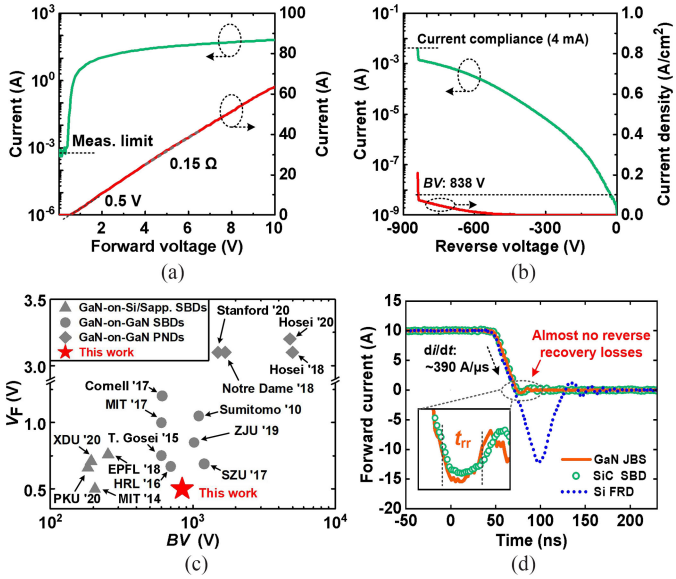

Fig. 2. (a) Forward and (b) reverse *I–V* characteristics in log scale and linear scale. (c) Benchmark of V_F versus BV of the GaN-on-GaN/Si/sapphire GaN SBDs and GaN PNDs. V_F values are extracted from the linear extrapolation of the forward current or at current density of 100 A/cm^2 [4]. (d) Reverse recovery characteristics of the GaN JBS diode and similar-rated commercial SiC SBD and Si FRD. Inset: Zoomed-in waveforms. t_{rr} is defined as the time when the reverse current recovers to 10% of its peak value. Q_{rr} is calculated by the time-integration of reverse current.

technology adoption [2]. Rugged avalanche capability and large surge current tolerance have been demonstrated, presenting a high avalanche energy of 57.8 mJ with BV of 965 V, and a high surge energy of 6.0 J with surge current of 65 A, obtaining a broad safety margin in reliability for the GaN diode. Besides, with the application and evaluation of the substrate thinning technique, heat accumulation effects have been identified as the dominant factor in determining the safety margin. This work thus clearly demonstrates the notable potentials of the sapphire-based quasi-vertical GaN JBS diodes in the low-cost, high-efficiency, and highly reliable power applications.

II. Device Fabrication and Characterizations

Fig. 1 shows the optical image and schematic cross-sectional view of the quasi-vertical GaN JBS diode fabricated on a 4-in C-face sapphire substrate consisting of 9-μm n$^-$-GaN drift layer and a 4-μm n$^+$-GaN current spreading layer. The 1.9-mm^2 device process begins with the formation of selective-area p-islands and junction termination extension regions based on magnesium (Mg) ion implantation by a proprietary technique [19], [20]. For the recovery of the lattice from the ion-implantation induced damage, and the removal of accumulated strain from the excess interstitial and vacancies, 1230 °C high-temperature postannealing process with 200-nm SiO_2 protective capping layer is conducted [19]. The mesa etching is performed after the removal of the SiO_2 capping layer. Then, the Schottky contact is formed with the Ni/Pt (300 nm/100 nm) stack, which is followed by the plasma-enhanced chemical vapor deposition of a 500-nm SiO_2 passivation layer [21]. Contact windows are then opened with dry etching, and the Ti/Al (200 nm/5 μm) stack is deposited to form both the field plate structure at the anode region and the ohmic contact on the highly doped n$^+$-GaN layer. Finally, in order to improve heat dissipation capability, technologies of substrate thinning and packaging have been implemented [22], obtaining a thinned substrate with the minimum thickness of 90 μm, which is the thickness limitation in our experiments without the wafer breakage. By using the high thermal conductivity soft solders [23], the diodes are mounted on a large copper plate, which is then encapsulated in a TO-220 package with epoxy molding compound.

Fig. 2(a) shows the pulsed forward *I–V* characteristics of the JBS diode, which exhibits a low forward turn-ON voltage (V_F) of 0.5 V as extracted from the linear extrapolation, and a high pulse current rectifying level up to 60 A (50-μs pulsewidth and 0.1% duty cycle), producing a low differential specific on-resistance (R_{on}) of 0.15 Ω. Meanwhile, highly uniform BV values near 838 V are obtained as defined at the leakage current of 0.1 A/cm^2 [4] [see Fig. 2(b)]. As shown in Fig. 2(c), the high BV with low V_F of the JBS diode in this work has outperformed the quasi-vertical GaN SBDs on foreign substrates [5], and approached the values of the vertical GaN-on-GaN SBDs [4], verifying the effectiveness of JBS structure in enhancing the reverse blocking performances [16].

To evaluate the dynamic switching performances of the fabricated GaN JBS diode, double-pulse-test measurements have been performed [24]. As shown in Fig. 2(d), under an extreme switching condition from a high forward current of 10 A to a reverse bias of 600 V with a di/dt of 390 A/μs, the GaN JBS diode exhibits fast reverse recovery performances with the reverse recovery time (t_{rr}) of ~11 ns and reverse recovery charge (Q_{rr}) of 3.5 nC, which is in the similar level with that of SiC SBD (C6D10065A, 650 V/10 A), presenting apparently lower switching loss than Si fast-recovery diode (FRD, RFV8TJ6SGC9, 600 V/8 A). This should be attributed to the high electron mobility and large critical electric field of GaN, as well as the relative immunity to surface-related charge trapping effects in the vertical structure [24]. These results thus indicate that the diodes are suitable for 600-V/10-A rating power rectifying applications.

III. Reliability Characterizations

A. Tests Setup

As shown in Fig. 3(a), the investigations on the avalanche ruggedness of the diodes are carried out by using the unclamped-inductive-switching (UIS) test setup [13], where the device

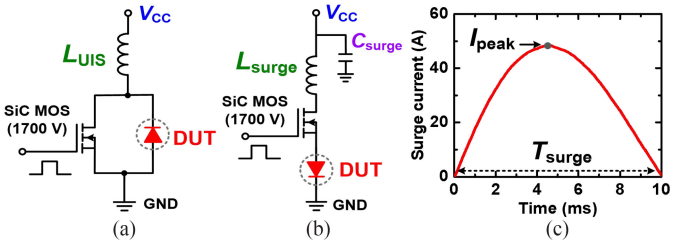

Fig. 3. DUT is reversely biased in the (a) UIS circuit and forwardly biased in the (b) surge current circuit. (c) Typical surge current waveform.

under test (DUT) is reversely biased and connected in parallel with a 1700-V/45-mΩ SiC MOSFET. In the test, the load inductor ($L_{\rm UIS}$) is first charged by the power supply ($V_{\rm CC}$) with the ON-state SiC MOSFET. Once the SiC MOSFET is turned OFF, the energy stored in $L_{\rm UIS}$ is forced to go through the DUT, driving it into breakdown state, whereby the BV and current are captured by the oscilloscope. By controlling a programmable pulse generator to adjust the ON/OFF state of the SiC MOSFET, the DUT could be driven into breakdown once-only or consecutively.

Fig. 3(b) shows the test setup for the surge current characterizations [14], consisting of the forwardly biased DUT in series with the SiC MOSFET and a resonant circuit module consisting of a load inductor ($L_{\rm surge}$) and a capacitor ($C_{\rm surge}$). When the SiC MOSFET is turned ON, the resonance circuit can generate a half-sine surge current pulse to go through the DUT. The typical surge current waveform is shown in Fig. 3(c), where the peak surge current ($I_{\rm peak}$) and the positive half-period of current pulse ($T_{\rm surge}$) are determined by [25]

$$I_{\rm peak} = V_{\rm CC}\sqrt{C_{\rm surge}/L_{\rm surge}} \tag{1}$$

$$T_{\rm surge} = \pi\sqrt{C_{\rm surge}L_{\rm surge}}. \tag{2}$$

B. Avalanche Ruggedness

Fig. 4(a) shows the UIS voltage and current waveforms of the JBS diode with $L_{\rm UIS} = 1$ mH and $V_{\rm CC} = 50$ V. The DUT voltage rapidly ramps to avalanche BV (∼965 V) with dV/dt of ∼6 V/ns after the SiC MOSFET turns OFF and gets clamped at this value for a duration of 11.4 μs due to the avalanche breakdown, whereas the DUT current gradually drops from 11.2 A to zero. The corresponding avalanche energy, calculated as the power-to-time integration, is as high as 57.8 mJ. To the best of our knowledge, this is the first demonstration of avalanche capability in the GaN JBS diode, and the sustained avalanche energy is comparable with the state-of-the-art GaN-on-GaN PNDs [13]. The demonstrated avalanche capability in the GaN JBS diode is ascribed to the modified peak electric field position from the Schottky contact interface to the bulk. Otherwise, the high critical electric field near 3 MV/cm for the onset of avalanche breakdown in GaN could induce severe barrier thinning effect in the Schottky junction and facilitate tunneling-dominated leakage.

In addition to single-pulse UIS event, continuously repeated UIS tests have been conducted to gain further insights of the device ruggedness under avalanche breakdown conditions [9]. As presented in Fig. 4(b), with avalanche energy of ∼57.8 mJ/pulse

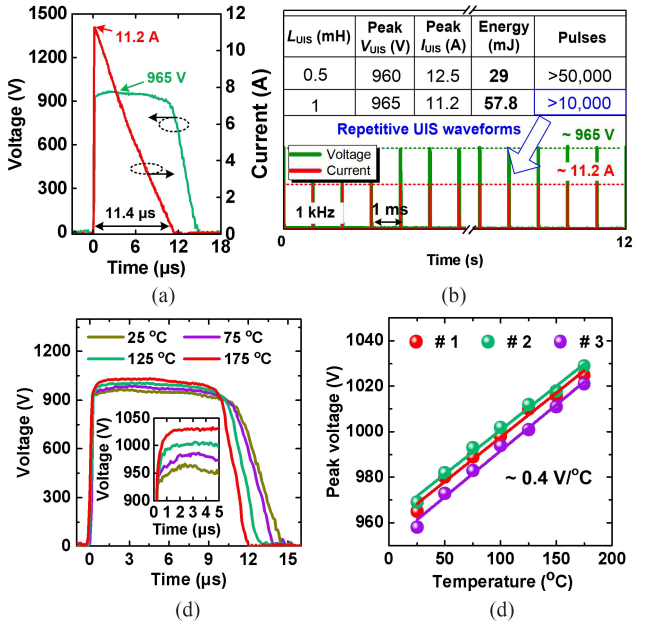

Fig. 4. (a) UIS waveforms with $L_{\rm UIS} = 1$ mH. (b) Summary of the repetitive avalanche parameters and waveforms. (c) UIS voltage waveforms at different temperatures. Inset: Zoomed-in view of the BV. (d) Positive temperature coefficient extracted from three samples.

obtained at $L_{\rm UIS}$ of 1 mH, the JBS diode can sustain over 10 000 continuous UIS pulses with a repeating frequency of 1 kHz, exhibiting no measurable degradation in I–V characteristics. For a lower $L_{\rm UIS}$ of 0.5 mH, similar BV and slightly higher peak avalanche current are observed, whereas the avalanche energy is reduced to 29 mJ/pulse with a decreased avalanche duration of ∼6 μs. Corresponding avalanche ruggedness is evidently enhanced with over 50 000 times repeatable breakdown, revealing the dominance of avalanche energy in the diodes avalanche ruggedness [26].

The DUT is then heated up by ceramic heating sheet and monitored by a thermocouple for the temperature-dependent UIS tests. As shown in Fig. 4(c), with the temperature rising from 25 to 175 °C, the BV increases from 965 to 1026 V. The enhanced BV at higher temperature should be a result of the thermally enhanced phonon scattering during the impact ionization [27], [28], further verifying the avalanche capability of the fabricated diode. The positive temperature coefficient as extracted from three identical samples is ∼0.4 V/°C [see Fig. 4(d)], being similar with the previously reported values [29]. It should be noted that the temperature-dependent UIS tests also present the reliability of the GaN diodes in up-to-175 °C high-temperature applications.

C. Surge Current Capability

In a forward surge transient, the large current flowing through the resistive diode can rapidly produce a huge amount of Joule heat [10], and then lead to an abrupt rise of the device temperature, which in turn would cause increased $R_{\rm on}$ and produce more Joule heat [30]. This positive feedback could generate severe heat accumulation effect and form localized hot spots

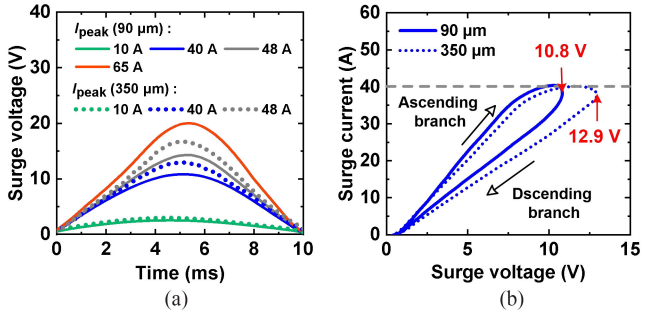

Fig. 5. (a) Surge voltage waveforms of the GaN SBD with 90- and 350-μm substrate thickness. (b) Corresponding surge I–V curves with $I_{\rm peak}$ of 40 A.

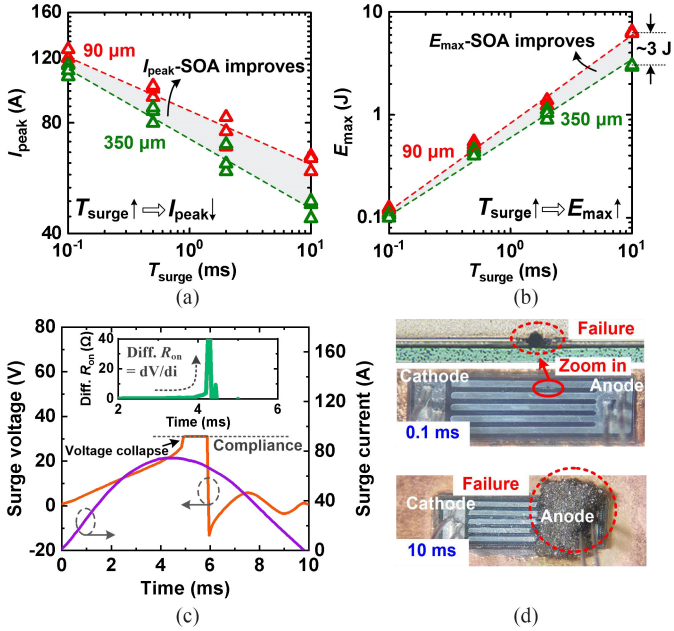

Fig. 6. (a) $I_{\rm peak}$- and (b) $E_{\rm max}$-SOA. (c) Typical failure waveforms during surge stress. (d) Failure profile in GaN SBD with $T_{\rm surge}$ of 0.1 and 10 ms.

inside the device, leading to the final failure [30]. Therefore, lowering the on-resistance of the diode is directly meaningful for enhancing the surge current capability. Meanwhile, to maximize the heat dissipation effect and to improve the surge capability, the sapphire substrate is herein thinned to ~90 μm [22], whereas control sample with normal substrate thickness of ~350 μm is also fabricated with the same TO-220 package. Fig. 5(a) presents the surge voltage waveforms of the diodes with different substrate thickness at $T_{\rm surge}$ of 10 ms. In both devices, the surge voltage is observed to increase with elevated $I_{\rm peak}$. But, the device with 90-μm substrate thickness can withstand a higher $I_{\rm peak}$ of 65 A, as compared to 48 A of the control sample. When comparing the surge I–V curves with an identical $I_{\rm peak}$ of 40 A, both diodes show similar variation trend, including the ascending and descending parts [see Fig. 5(b)], where the current dispersion between the two parts should be a result of heat accumulation effect during the surge event, which then leads to the rise of conduction resistance. Moreover, it is found that the device with 90-μm-thickness substrate exhibits apparently smaller peak voltage (10.8 V), indicating the alleviated rise in $R_{\rm on}$.

By adjusting $L_{\rm surge}$ or $C_{\rm surge}$, the current surging performance at different $T_{\rm surge}$ can be obtained based on (2). Also, the maximum energy ($E_{\rm max}$) dissipation of the devices can be calculated based on the power-to-time integration. Correspondingly, $T_{\rm surge}$-dependent $I_{\rm peak}$ and $E_{\rm max}$ SOA are plotted in Fig. 6(a) and (b), respectively. With an increased surging duration, $I_{\rm peak}$ decreases but still generate an enhanced surging energy, being increased from 0.1 to 6.0 J at $T_{\rm surge}$ of 0.1 and 10 ms, respectively. Meanwhile, the JBS diodes with 90-μm substrate thickness show a broader current/energy SOA than that of the control samples, especially at higher $T_{\rm surge}$ where the energy difference reaches ~3.0 J. These results clearly present the effectiveness of substrate thinning of sapphire in obtaining lower $R_{\rm on}$ degradation and higher current surging capability by facilitating the heat dissipation.

Fig. 6(c) shows the typical failure surge waveforms with a large $I_{\rm peak}$ up to ~7.5× the rated current (10 A) of the GaN JBS diode, where the collapse of voltage drop is observed. The transient thermal accumulation results in an evidently enhanced differential $R_{\rm on}$ [see the inset in Fig. 6(c)], accelerating the devices destruction. Further decapsulation experiment has been carried out to identify the failure position [see Fig. 6(d)]. The initial failure spot locates at the sidewall of the multifinger anode electrode with $T_{\rm surge}$ of 0.1 ms, and spreads to the whole anode region with $T_{\rm surge}$ increased to 10 ms, resulting in the catastrophic thermal destruction. Accordingly, heat accumulation effect during the surge event that elevates the p–n junction temperature underneath the anode edge to the melting temperature of aluminum pad is considered as the root of the device failure [31], revealing the significance of thermal management in the sapphire-based GaN JBS diodes.

IV. Conclusion

In this letter, based on the Mg-ion implanted termination technology, selective p-type islands underneath the Schottky contact of the GaN JBS diode are demonstrated. Correspondingly, the diode achieves excellent performances in both static and dynamic characterizations, especially the 600-V/10-A rectifying capability. More importantly, after implementing the high-performance diodes into the inductive load circuits, high transient immunity is observed incorporating both robust avalanche breakdown capacity and surge current tolerance, obtaining a large SOA for the fabricated GaN diode. These results thus present the large potentials of the sapphire-based quasi-vertical GaN JBS diodes in high-efficiency, high-power, and highly reliable power applications.

References

[1] Y. F. Wu, J. Gritters, L. Shen, R. P. Smith, and B. Swenson, "kV-class GaN-on-Si HEMTs enabling 99% efficiency converter at 800 V and 100 kHz," *IEEE Trans. Power Electron.*, vol. 29, no. 6, pp. 2634–2637, Jun. 2014.

[2] K. J. Chen *et al.*, "GaN-on-Si power technology: Devices and applications," *IEEE Trans. Electron Devices,* vol. 64, no. 3, pp. 779–795, Mar. 2017.

[3] L. Nela, R. Van Erp, G. Kampitsis, H. K. Yildirim, J. Ma, and E. Matioli, "Ultra-compact, high-frequency power integrated circuits based on GaN-on-Si Schottky barrier diodes," *IEEE Trans. Power Electron.,* vol. 36, no. 2, pp. 1269–1273, Feb. 2021.

[4] S. Han, S. Yang, and K. Sheng, "Fluorine-implanted termination for vertical GaN Schottky rectifier with high blocking voltage and low forward voltage drop," *IEEE Electron Device Lett.,* vol. 40, no. 7, pp. 1040–1043, Jul. 2019.

[5] Y. Li *et al.*, "Quasi-vertical GaN Schottky barrier diode on silicon substrate with 10^{10} high on/off current ratio and low specific on-resistance," *IEEE Electron Device Lett.,* vol. 41, no. 3, pp. 329–332, Mar. 2020.

[6] C. De Santi, M. Meneghini, G. Meneghesso, and E. Zanoni, "Review of dynamic effects and reliability of depletion and enhancement GaN HEMTs for power switching applications," *IET Power Electron.,* vol. 11, no. 4, pp. 668–674, Oct. 2018.

[7] B. Shankar, A. Soni, S. Raghavan, and M. Shrivastava, "Trap-assisted and stress induced safe operating area limits of AlGaN/GaN HEMTs," *IEEE Trans. Device Mater. Rel.,* vol. 20, no. 4, pp. 767–774, Dec. 2020.

[8] B. Shankar *et al.*, "Time dependent shift in SOA boundary and early breakdown of epi-stack in AlGaN/GaN HEMTs under fast cyclic transient stress," *IEEE Trans. Device Mater. Rel.,* vol. 20, no. 3, pp. 562–569, Jul. 2020.

[9] X. Zhou *et al.*, "A deep insight into the degradation of 1.2kV 4H-SiC MOSFETs under repetitive unclamped inductive switching stresses," *IEEE Trans. Power Electron.,* vol. 33, no. 6, pp. 5251–5261, Jun. 2018.

[10] E. Van Brunt, T. Barbieri, A. Barkley, J. Solovey, J. Richmond, and B. Hull, "Surge current failure mechanisms in 4H-SiC JBS rectifiers," in *Proc. IEEE Int. Symp. Power Semicond. Devices IC's*, May 2018, pp. 415–418.

[11] B. Shankar, A. Soni, H. Chandrasekar, S. Raghavan, and M. Shrivastava, "First observations on the trap-induced avalanche instability and safe operating area concerns in AlGaN/GaN HEMTs," *IEEE Trans. Electron Devices,* vol. 66, no. 8, pp. 3433–3440, Aug. 2019.

[12] B. Shankar *et al.*, "On the trap assisted stress induced safe operating area limits of AlGaN/GaN HEMTs," in *Proc. IEEE Int. Rel. Phys. Symp.*, Mar. 2018, pp. 4E.4-1–4E.4-5.

[13] J. Liu *et al.*, "Trap-mediated avalanche in large-area 1.2 kV vertical GaN p-n diodes," *IEEE Electron Device Lett.,* vol. 41, no. 9, pp. 1328–1331, Sep. 2020.

[14] S. W. Han, S. Yang, Y. K. Li, Y. X. Liu, and K. Sheng, "Photon-enhanced conductivity modulation and surge current capability in vertical GaN power rectifiers," in *Proc. IEEE Int. Symp. Power Semicond. Devices IC's*, May 2019, pp. 63–66.

[15] S. Duguay, A. Echeverri, C. Castro, and O. Latry, "Evidence of Mg segregation to threading dislocation in normally-off GaN-HEMT," *IEEE Trans. Nanotechnol.,* vol. 18, no. 1, pp. 995–998, Sep. 2019.

[16] Y. Zhang *et al.*, "Vertical GaN junction barrier Schottky rectifiers by selective ion implantation," *IEEE Electron Device Lett.,* vol. 38, no. 8, pp. 1097–1100, Aug. 2017.

[17] W. Li *et al.*, "Design and realization of GaN trench junction-barrier-Schottky-diodes," *IEEE Trans. Electron Devices,* vol. 64, no. 4, pp. 1635–1641, Apr. 2017.

[18] S. Abhinay *et al.*, "Improved breakdown voltage in vertical GaN Schottky barrier diodes on free-standing GaN with Mg-compensated drift layer," *Japanese J. Appl. Phys.,* vol. 59, no. 1, Dec. 2019, Art. no. 010906.

[19] Y. T. Shi *et al.*, "Realization of p-type gallium nitride by magnesium ion implantation for vertical power devices," *Sci. Rep.,* vol. 9, no. 1, Jun. 2019, Art. no. 8796.

[20] W. Xu *et al.*, "Magnesium ion-implantation-based gallium nitride p-i-n photodiode for visible-blind ultraviolet detection," *Photon. Res.,* vol. 7, no. 8, pp. B48–B54, Aug. 2019.

[21] Y. Lu *et al.*, "Multi-aperture anode based AlGaN/GaN Schottky barrier diodes with low turn-on voltage and high uniformity," *Appl. Phys. Exp.,* vol. 13, no. 9, Aug. 2020, Art. no. 096502.

[22] R. Rupp, R. Gerlach, U. Kirchner, A. Schlögl, and R. Kern, "Performance of a 650V SiC diode with reduced chip thickness," *Mater. Sci. Forum,* vol. 717–720, pp. 921–924, May 2012.

[23] V. R. Manikam and C. Kuan Yew, "Die attach materials for high temperature applications: A review," *IEEE Trans. Compon., Packag. Manuf. Technol.,* vol. 1, no. 4, pp. 457–478, May 2011.

[24] S. Han, S. Yang, R. Li, X. Wu, and K. Sheng, "Current-collapse-free and fast reverse recovery performance in vertical GaN-on-GaN Schottky barrier diode," *IEEE Trans. Power Electron.,* vol. 34, no. 6, pp. 5012–5018, Jun. 2019.

[25] Y. Liu, S. Yang, S. Han, and K. Sheng, "Investigation of surge current capability of GaN E-HEMTs in the third quadrant: The impact of P-GaN contact," *IEEE J. Emerg. Sel. Topics Power Electron.,* vol. 7, no. 3, pp. 1465–1474, Sep. 2019.

[26] W. Liu *et al.*, "Avalanche ruggedness of GaN p-i-n diodes grown on sapphire substrate," *Physica Status Solidi*, vol. 215, no. 18, Jun. 2018, Art. no. 1800069.

[27] I. C. Kizilyalli, A. P. Edwards, H. Nie, D. Disney, and D. Bour, "High voltage vertical GaN p-n diodes with avalanche capability," *IEEE Trans. Electron Devices,* vol. 60, no. 10, pp. 3067–3070, Oct. 2013.

[28] T. Maeda *et al.*, "Measurement of avalanche multiplication utilizing Franz-Keldysh effect in GaN p-n junction diodes with double-side-depleted shallow bevel termination," *Appl. Phys. Lett.,* vol. 115, no. 14, Sep. 2019, Art. no. 142101.

[29] C. De Santi *et al.*, "Demonstration of avalanche capability in polarization-doped vertical GaN pn diodes: Study of walkout due to residual carbon concentration," in *Proc. IEEE Int. Electron Devices Meeting*, Dec. 2018, pp. 30.2.1–30.2.4.

[30] J. León *et al.*, "Temperature effects on the ruggedness of SiC Schottky diodes under surge current," *Microelectron. Rel.,* vol. 54, no. 9/10, pp. 2207–2212, Aug. 2014.

[31] N. Ren, J. Wu, L. Liu, and K. Sheng, "Improving surge current capability of SiC merged PiN Schottky diode by adding plasma spreading layers," *IEEE Trans. Power Electron.,* vol. 35, no. 11, pp. 11316–11320, Nov. 2020.